International Journal of Biochemistry and Cell Biology 114 (2019) 105570

Contents lists available at ScienceDirect

International Journal of Biochemistry and Cell Biology

journal homepage: www.elsevier.com/locate/biocel

Human keratinocyte-derived microvesicle miRNA-21 promotes skin wound healing in diabetic rats through facilitating fibroblast function and angiogenesis

Qian Li[b], Hui Zhao[a], Weimin Chen[a], Ping Huang[a,*], Jiarui Bi[c]

[a] Department of Stomatology, Tongji Hospital, Tongji Medical College, Huazhong University of Science and Technology, Wuhan, China
[b] Department of Radiology, Tongji Hospital, Tongji Medical College, Huazhong University of Science and Technology, Wuhan, China
[c] Faculty of Dentistry, Department of Oral Biological and Medical Sciences, University of British Columbia, Vancouver, BC, Canada

ARTICLE INFO

Keywords:
Microvesicle
miR-21
Wound healing
Fibroblast migration
Angiogenesis

ABSTRACT

Skin wound healing is a complex physiological process that maintains the integrity of the skin tissues, involving a variety of distinct cell types and signaling molecules. The specific signaling pathways or extracellular cues that govern the healing processes remain elusive. Microvesicles (MVs) have recently emerged as critical mediators of cell communication by delivery of genetic materials to target cells. In this study, we found the direct delivery of HEKa-MVs expressing miR-21 mimics significantly promoted the healing of skin wound in diabetic rats. In-depth studies showed that MV miR-21 promoted fibroblast migration, differentiation, and contraction, induced a pro-angiogenic process of endothelial cells and mediated a pro-inflammatory response. Mechanically, MV miR-21 might target specific essential effector mRNA in fibroblasts such as MMP-1, MMP-3, TIMP3, and TIMP4 to increase MMPs expression and enzymatic activities. Moreover, MV miR-21 regulated α-SMA and N-cadherin to induce fibroblast-myofibroblast differentiation. MV miR-21 up-regulated the IL-6 and IL-8 expressions and their secretion to amplify the immune response. Furthermore, MV miR-21 down-regulated PTEN and RECK in protein level, and activate MAPK/ERK signaling cascade, thereby promoting fibroblast functions. Thus, our study has provided for the first time the basis for the potential application of HEKa-MVs, and MV miR-21 in particular for wound healing.

1. Introduction

Diabetes as one of the most common and serious complications affects 340 million people in the world (Whiting et al., 2011). One of the most severe symptoms of diabetes is the inability in wound healing (Bloomgarden et al., 2015; Geach, 2015; Long et al., 2016; Salazar et al., 2016). Approximately 25% of diabetic patients suffer from diabetic lower-extremity ulcer throughout their lives. These wounds with slow healing and frequent reoccurrence, increase the risk of infection and the need for amputation (Gao et al., 2015; Ke et al., 2015; Wong et al., 2015; Zheng et al., 2015). The skin wound healing has been widely studied to develop novel treatment modality for wound healing in diabetic patients. The process of wound healing in skin consists of keratinocyte proliferation, extracellular matrix (ECM) remodeling, and angiogenesis (Sorg et al., 2017). The proliferative phase fills up the defective skin through serving to re-epithelialization, granulation tissue formation, and restore the vascular network restoration (Kalucka et al., 2013; Steinstraesser et al., 2014; Yang et al., 2017). During the ECM remodeling, fibroblasts migrate and proliferate at the wound site and synthesize ECM such as collagen and fibronectin for ECM fibers generation and rearrangement (Govindaraju et al., 2018; Scherer et al., 2009). Fibroblasts also secrete growth factors to stimulate and promote angiogenesis at the wound regions to facilitate wound repair (Johnson and Wilgus, 2014). Despite these important findings, the specific signaling pathways or extracellular cues that coordinate the complex network of healing processes have remained elusive. Recent studies have suggested that the collaborative dermal–epidermal crosstalk between fibroblasts and keratinocytes play a key role in the healing of skin wound (Bassino et al., 2017; Brauchle et al., 2017; Guzman-Uribe et al., 2017; Werner et al., 2007). During the re-epithelialization phase of wound healing, keratinocytes-derived signals are required for dermal fibroblasts to reestablish a functional epidermis mainly through a paracrine mechanism (Ghaffari et al., 2009; Harrison et al., 2006). The signaling mediators of fibroblast–keratinocyte interaction include

* Corresponding author at: Department of Stomatology, Tongji Hospital, Tongji Medical College, Huazhong University of Science and Technology, No. 1095 Jiefang Road, Wuhan, Hubei, 430030, China.
E-mail address: huangping_hust@hotmail.com (P. Huang).

https://doi.org/10.1016/j.biocel.2019.105570
Received 18 February 2019; Received in revised form 24 May 2019; Accepted 7 July 2019
Available online 11 July 2019
1357-2725/

secreted cytokines such as keratinocyte growth factor (KGF), platelet-derived growth factor (PDGF) and transforming growth factor (TGF)-β (Menon et al., 2012). Furthermore, keratinocytes and fibroblasts co-operatively induce collagen synthesis and contraction *in vitro* (Schafer et al., 1989; Souren et al., 1989).

Microvesicles (MVs), a membrane lipid vesicle with a diameter of 100–1000 nm, mediate cell paracrine action by transferring genetic materials and proteins to target cells (Bi et al., 2016; Huang et al., 2015). A variety of cells, including epithelial cells, secrete MVs under both normal and pathophysiological conditions (Bi et al., 2016; Huang et al., 2015; Van Niel et al., 2001). The function of MVs is believed depending on the host cell type which they originate from, and they carry the cargo by traveling in particular distances to the target cells through biological fluids (Bi et al., 2016; Lee et al., 2011). There is growing evidence implicating the involvement of MVs in wound healing (Huang et al., 2015; Staals and Pruijn, 2010). Recently, we have shown that the MVs derived from keratinocytes play a profound role in fibroblast-mediated wound healing in skin and oral cavity (Bi et al., 2016; Huang et al., 2015). Keratinocyte-derived MVs regulated fibroblast gene expressions *via* activating ERK1/2, JNK, Smad, and p38 signaling pathways and promoted fibroblast cell migration and fibroblast-initiated angiogenesis (Bi et al., 2016; Huang et al., 2015). The precise underlying mechanism has, however, remained unclear.

MicroRNAs (miRs), with their substantial effects on target gene expression, have emerged as key players in various biological processes, especially in wound healing (Baumann and Winkler, 2014; Meng et al., 2018). miR-21, the most frequently upregulated miR in human cancers and other diseases, was highly implicated in many cellular processes, including cell proliferation, differentiation, migration, apoptosis, and epithelial to mesenchymal transition (EMT) (Krichevsky and Gabriely, 2009). Of interest, miR-21 was reported to be elevated in keratinocytes following skin injury, which was coincident with the temporal expression of TGF-β1, a critical mediator of wound healing (Long et al., 2018; Wang et al., 2012; Yang et al., 2011). Importantly, TGF-β1 upregulated miR-21, which was, in turn, essential for TGF-β-driven keratinocyte migration (Long et al., 2018; Wang et al., 2012; Yang et al., 2011). Thus, miR-21 downstream of TGF-β signaling could be an important mediator of wound healing. However, the function of miR-21 in the healing of the diabetic wound is largely unknown.

In this study, we investigated whether and how keratinocyte-derived MV miR-21 was involved in the diabetic wound healing *in vivo* and *in vitro*. We were able to show that the direct delivery of keratinocyte-derived MVs expressing miR-21 mimics significantly promoted the healing of skin wound in diabetic rats. We showed that MV miR-21 regulated the expression of wound healing-associated genes and effect on the cell behavior of fibroblasts *via* the activation of MAPK/ERK signaling. The findings show a potential role of keratinocyte-derived MVs and MV miR-21 in diabetic wound healing.

2. Materials and methods

2.1. Cell lines, antibodies, and reagents

Human foreskin fibroblast (HFF-1) and human epidermal keratinocyte adult (HEKa) were obtained from ScienCell (San Diego, CA, USA). HFF-1 was maintained in DMEM (ThermoFisher Scientific, Shanghai, China) with 10% heat-inactivated FBS (TBD, Tianjin, China) and 1% penicillin-streptomycin (Beyotime Biotechnology, Shanghai, China) at 37 °C in a humidified atmosphere of 5% CO_2. HEKa was cultured in RPMI 1640 (ThermoFisher Scientific, Shanghai, China) with the same conditions as HFF-1. Antibodies against α-SMA, cadherin-2, PTEN, RECK, ERK1/2, phospho-ERK1/2, VEGF, and β-actin were purchased from Cell Signaling Technology (Danvers, MA, USA). Rho inhibitor Y-27632 was obtained from Selleckchem (Shanghai, China), while streptozotocin (STZ) was purchased from Sigma-Aldrich (St. Louis, MO, USA). The information of antibodies used in the study is listed in Table 1.

Table 1
List of antibodies used for immunocytochemistry and Western blotting.

Antibody	Manufacturer	Host	Dilution
Anti-α-SMA	ab5694	Rabbit	1:5000
Anti-Cadherin-2	ab76011	Rabbit	1:5000
Anti-β-Actin	ab8227	Rabbit	1:5000
Anti-PTEN	ab170941	Rabbit	1:1000
Anti-RECK	ab115844	Rabbit	1:5000
Anti-ERK1/2	ab184699	Rabbit	1:1000
Anti-phospho-ERK1/2	ab214362	Rabbit	1:2000
Anti-VEGF	ab39638	Rabbit	1:1000

HRP-conjugated goat polyclonal secondary antibody to mouse and rabbit (1:10,000).

2.2. Stable miR-21 mimic and inhibitor HEKa transfectants

Lentiviral transfer plasmids encoding miR-21 mimic and inhibitor were obtained from GenePharma (Shanghai, China). To package lentivirus expressing miR-21 mimics and inhibitors, the respective transfer plasmids were individually co-transfected with the packaging vector into HEK293FT cells using Lipofectamine 2000 (Invitrogen, Carlsbad, CA). Empty vector without miR-21 mimics or inhibitors was transfected as control. After 48 h, the culture medium was collected for the harvest of packaged lentiviruses, of which the titers were quantitatively determined. To stably express miR-21 mimic and inhibitor in HEKa cells, 6×10^5 cells were transduced with respective lentiviruses with an MOI of 40. After 24 h, the cells were washed twice with phosphate buffer saline (PBS), and medium supplemented with puromycin (5 μg / mL) was replenished for stable cell selection.

2.3. MV collection

MVs were collected as previous described (Bi et al., 2016; Huang et al., 2015). HEKa cells with or without miR-21 mimic or miR-21 inhibitor were cultured for 48 h in complete DMEM medium with 10 μM Y-27632 to prevent keratinocyte terminal differentiation (Chapman et al., 2010). Confluent HEKa cells were washed thrice with PBS and then cultured in serum-free DMEM with 10 μM Y-27632 for another 48 h. Conditioned medium from the cultures was centrifuged (Allegra 64R, Beckman Coulter, Shanghai, China) at + 4 °C at 3000 *g* for 15 min to remove cell debris following with centrifuging at 25,000 *g* for 30 min to collect MVs. The collected MVs pellets were rinsed with PBS, homogeneously re-suspended in FBS-free medium, and kept on ice until used. Total MV protein content was measured using Bio-Rad protein assay (Bio-Rad, Life Science, Shanghai, China).

2.4. Scan transmission electron microscopy

Scan transmission electron microscopy was performed as previously described (Bi et al., 2017). Collected MVs were resuspended in 2.5% glutaraldehyde (Beyotime Biotechnology) in 0.1 M PIPES [piperazine-1,4-bis (2-ethane sulfonic acid)] buffer pH 7.4 (Beyotime Biotechnology). A drop of resuspended MVs was placed on a 200 mesh formvar-coated copper grid and negatively stained with 2% aqueous uranyl acetate (Beyotime Biotechnology). The MVs were imaged at 30 KeV in STEM mode with a segmented solid-state STEM detector in bright-field mode (Helios 650 Nanolab, FEI, Hillsboro, OR, USA). Images were captured using MAPS software (FEI) for automated acquisition of high-resolution images from large areas; in this case, 73 x 49 μm was analyzed with a 7-mm pixel resolution. The stitched image was saved as a TIFF file and analyzed using ImageJ software (imagej.nih.gov).

2.5. Migration assay

Sterile 12 mm coverslips were first coated with 0.2% gelatin solution (Fisher Scientific) at +37 °C for 1 h, followed by cross-linking with 1% glutaraldehyde solution for 30 min. HFF-1 (50,000 per well) was seeded on the coverslips and cultured in culture medium with 10% FBS for 24 h following with serum-starved for another 24 h. The cultures were then wounded with a sterile pipette tip and treated with 2 μg MVs collected from normal or transfected HEKa (empty vector, miR-21 mimic or mir-21 inhibitor) for 10 h. Cell migration was observed every 2 h and images were taken using Nikon Eclipse TS100 microscope (Nikon) with Nikon Coolpix 995 camera (Nikon). A set of samples were fixed and stained with 1% crystal violet (Sigma) at the timepoint of 0 h and 10 h.

2.6. Tube formation assay

HFF-1 were seeded in 6-well plates (2×10^5 cells per well) for two days. HFF-1 was then rinsed with sterile PBS and treated with 2 μg / mL respective MVs in FBS-free medium for another two-day incubation. All medium were collected, first spun at 3000 g at +4 °C for 15 min to remove cell debris, and then concentrated using Amicon Ultra Centrifugal Filters (Millipore Ireland Ltd, Tullagreen, Carrigtwohill CO, CORK IRL). For the assay, 96-well plate was coated with 30 μL of Geltrex LDEV-free basement membrane extract (Gibco) per well. HUVECs (human umbilical vein endothelial cell, Gibco) were maintained in Medium 200 (Gibco) supplemented with LSGS (low serum growth supplement, Gibco) and antibiotics (100 U / mL penicillin, 100 U / mL streptomycin sulfate; TBD C0222). For the experiment, HUVECs (40,000 per well) were seeded in 100 μL of fibroblast conditioned medium into the precoated 96-well plate and incubated overnight. Endothelial tube formation was quantified using digital images of the wells.

2.7. The diabetic rat model of skin wound

Animals were maintained according to protocols approved by the Institutional Animal Care and Use Committee, Huazhong University of Science and Technology (Hubei, China; IACUC ID: 2014S652). During experimentation, all mice were kept in the animal center of the Tongji Medical College, Huazhong University of Science and Technology under specific pathogen-free (SPF) conditions (License Number: SYXK#2016-0057). Male Sprague-Dawley rats (6–8 weeks old), purchased from Nanjing Biomedical Research Institute of Nanjing University, were kept in a humidity-controlled facility with a 12 -h light/dark cycle at ambient temperature (25℃). Rats were given *ad libitum* access to sterilized chow and water. Diabetes was induced in rats (weighted 180 to 220 g) by an intraperitoneal injection of 30 mg / kg STZ in 2% sodium citrate buffer (pH 4.5) after overnight fasting. Diabetic rats showed elevated blood glucose (*i.e.*, > 16.65 mmol/L), strong positive glycosuria and clinical symptoms (*i.e.*, thinned skin and weight loss). A full-thickness cutaneous wound in 2.54 cm^2 round area was created on the back of the rat under the anesthetization with pentobarbital sodium (30 mg/kg, *i.p.*).

Diabetic rats with cutaneous wound were randomly assigned into 4 different groups: (i) 200 μL PBS (n = 3); (ii) 2 μg MVs with empty vector (n = 3); (iii) 2 μg MVs with miR-21 mimics (n = 3); and (iv) 2 μg MVs with miR-21 inhibitor (n = 3). PBS or MVs were applied at the edge of the cutaneous wound three days after the injury was created. At day 4, 7, 11, 14, 17, 21 post-wounding, wounds were digitally photographed with an Olympus SP-800 UZ camera. The area of the wound was measured by digital planimetry using ImageJ software version 2.1.4.6 (NIH, Bethesda, MD, USA). At day 21, wound tissues were collected for western blotting, Haematoxylin and eosin (H&E) staining and Masson's staining (Masson staining kit; Leagene, Beijing, China).

2.8. Immunohistochemistry

Collected skin tissue sections of the rat were deparaffinized in xylene, rehydrated through graded ethanol and then boiled for 30 min in citrate buffer (10 mM, pH 6.0) for antigen retrieval. Endogenous peroxidase activity was inhibited by 3% hydrogen peroxide for 30 min; samples were then blocked with 5% bovine serum albumin (BSA; Boster Biological Technology, China) and incubated with diluted primary antibody against VEGF (abcam, Shanghai, China) for 12 h at 4 °C followed by secondary antibody (abcam, Shanghai, China) for 20 min at 37 °C. Finally, the slides were visualized with 3,3′-diaminobenzidine (DAB; Boster Biological Technology, China) and counterstained with hematoxylin for microscopic observation.

2.9. RT-qPCR and western blotting

Fibroblasts HFF-1 were treated with different types of MVs for 24 h (for total RNA isolation) or 48 h (for protein isolation) in a serum-free medium. Expression of wound healing-associated genes and proteins were analyzed using RT-qPCR and western blotting, respectively, as previously described (Bi et al., 2018, 2017). The information of primers for RT-qPCR used in this study are listed in Table 2. Actin and U6 were used as housekeeping genes in the analysis. To assess the activation of cellular signaling pathways, HFF-1 cells were starved in a serum-free medium for 2 h following with MV treatment for 15 min., based on previously described (Bi et al., 2016; Huang et al., 2015). The activation of ERK1/2 signaling was then analyzed by western blotting.

3. ELISA

ELISA was performed as previously described (Bi et al., 2016; Huang et al., 2015). To examine the effect of MVs on the release of IL-6 and IL-8 from fibroblasts, HFF-1 cells were seeded in 6-well plates (2×10^5 cells per well), cultured for two days and then treated with respective MVs (2 μg/mL) for another two days. IL-6 and IL-8 in the collected culture medium were determined using human IL-6 and IL-8 ELISA kits (R&D Systems, Minneapolis, MN).

3.1. Statistical analysis

Statistical software GraphPad Prism version 4.0 (GraphPad Software Inc., San Diego, CA, USA) was used for data analysis. All experiments

Table 2
Primers used for RT-qPCR.

Target	Primer sequence	Orientation	Amplicon (bp)
miR-21	CGGTAGCTTATCAGACTG	Forward	53
	GAGCAGGCTGGAGAA	Reverse	
MMP-1	TGAAGAATGATGGGAGGCAAG	Forward	168
	ACTGAGCCACATCAGGCACTC	Reverse	
MMP-3	TGGCATTCAGTCCCTCTATGG	Forward	147
	ATTTCTCCCCTCAGAGTGCTG	Reverse	
TIMP-3	CGCAAGGGGCTGAACTATC	Forward	156
	GGCGTAGTGTTTGGACTGGTAG	Reverse	
TIMP-4	CCCTAACGAGTGCCTCTGGAC	Forward	151
	AACGATGTCAACAAACTCCTTCC	Reverse	
α-SMA	TGTACCCTGGGATCGCTGAC	Forward	179
	CTCGTCGTACTCCTGCTTGG	Reverse	
Cadherin-2	GATCCTACTGGACGGTTCGC	Forward	155
	GGGTGCTGAATTGCCCTTG	Reverse	
IL-6	AAAGCAGCAAAGAGGCACTG	Forward	137
	TACCTCAAACTCCAAAAGACCAG	Reverse	
IL-8	GACATACTCCAAACCTTTCCACC	Forward	162
	AACTTCTCCACAACCCTCTGC	Reverse	
Actin	TGACGTGGACATCCGCAAAG	Forward	205
	CTGGAAGGTGGACAGCGAGG	Reverse	
U6	CTCGCTTCGGCAGCACATA	Forward	92
	CGCTTCACGAATTTGCGTG	Reverse	

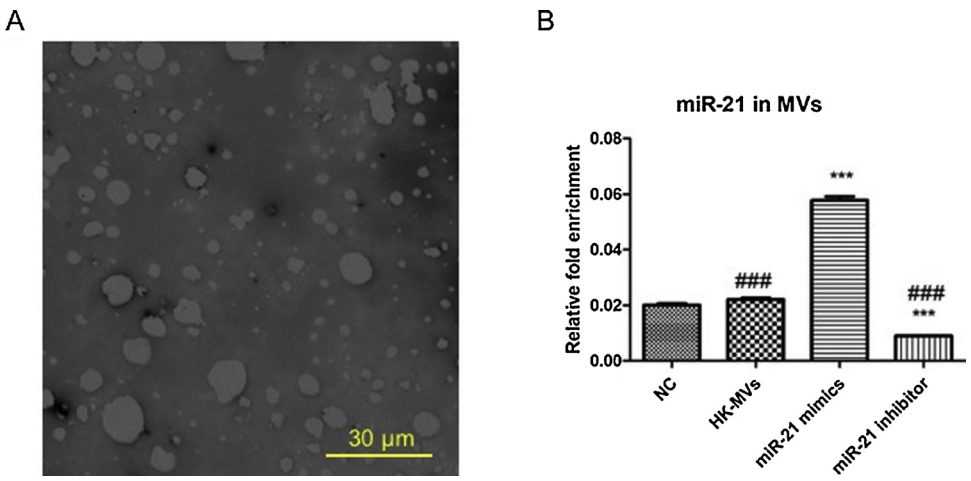

Fig. 1. Morphology and miR-21 expression of keratinocyte-derived MVs (A) STEM image of HEKa-MVs. Bar = 30 μm. (B) The expression of miR-21 in MVs derived from HEKa was analyzed by RT-qPCR. The results show mean ± SEM from triplicate experiments (***, $P < 0.001$ comparing to HEKa-MVs group. $^{###}$, $P < 0.001$ comparing to miR-21 mimic group).

were repeated separately at least three times, and data were expressed as the mean ± standard error of the mean (SEM). Student's *t*-test and one-way ANOVA with Tukey's post hoc test was performed for paired comparisons and multiple comparisons, respectively ($p < 0.05$). RT-qPCR data were analyzed using log2-transformed data.

4. Result

4.1. Morphology and miR-21 expression of keratinocyte-derived MVs

MVs derived from keratinocyte HEKa cells were isolated and purified by a series of low-speed centrifugation and ultracentrifugation, and the morphology of the isolated MVs was confirmed using STEM. The result showed that the HEKa-MVs displayed a round morphology in the range of 1 to 0.5 μm (Fig. 1A), which was similar to previously described (Bi et al., 2016; Hu et al., 2018; Huang et al., 2015). miR-21 was detected in HEKa-MVs by agarose gel electrophoresis (data not shown). The expression of miR-21 in different MVs was studied using real-time PCR. Normal HEKa-MVs and MVs from HEKa infected with virus carrying the empty vector only (Vector) showed a similar level of miR-21 expression (Fig. 1B). Comparing to the vector MVs, the MVs from miR-21 mimic infected HEKa (miR-21 mimic) had significantly higher expression of miR-21, while the MVs from miR-21 inhibitor infected HEKa (miR-21 inhibitor) showed lower expression of miR-21 (Fig. 1B).

4.2. MV miR-21 promoted fibroblast migration and fibroblast-mediated angiogenesis

To investigate whether MV miR-21 plays a key mediation function in fibroblast-keratinocyte crosstalk during the wound healing process, we examined whether miR-21-containing MVs derived from keratinocytes would role in fibroblast ECM remodeling and fibroblast-mediated angiogenesis. The migration ability of fibroblasts after MV treatment was assessed using the wound-healing assay. Results showed that in contrast to vector MVs, treatment with MVs overexpressing miR-21 mimic significantly accelerated wound closure of HFF-1 cells at 24 h and 48 h after scratching, while the pro-migratory effect was attenuated by miR-21 inhibitor MVs (Fig. 2A and B). We also tested the contraction activity of fibroblasts with the treatment of empty vector, miR-21 mimic or miR-21 inhibitor MVs by fibroblast-collagen gel contraction assay (Huang et al., 2015). However, neither the miR-21 mimic nor miR-21 inhibitor MVs did not regulate collagen gel contraction, which was consistent with the previous observation (data not shown) (Huang et al., 2015).

Next, we investigated the influence of MV miR-21 on the angiogenic activity of endothelial cells by the tube formation assay of HUVEC. Tube formation of HUVEC was significantly increased by the culture medium of fibroblast with MVs (Fig. 2C). miR-21 mimic MVs increased both the number and relative length of branches compared to vector MVs and miR-21 inhibitor MVs (Fig. 2D and E). However, it showed no significant differences between miR-21 inhibitor MVs and vector MVs in the number and relative length of branches of HUVEC tube formation.

4.3. MV miR-21 promoted diabetic cutaneous wound healing in the rat model

We next investigated the *in vivo* effect of miR-21 containing MVs on the healing of the cutaneous wound in diabetic rats. Treatment with miR-21 mimic MVs dramatically accelerated wound healing process as revealed by the progressively smaller wound areas measured at day 7, 11, 14 and 17 post-wounding, comparing to treatments with PBS, vector MVs, and miR-21 inhibitor MVs (Fig. 3A and B). At day 21, complete wound closure was observed in rat with the treatment of the miR-21 mimic MVs, while the rats treated with PBS, vector MVs, and miR-21 inhibitor MVs remained scar in the areas (Fig. 3A and B). Consistent with the results of tube formation of HUVEC, the wounds treated with miR-21 mimic MVs exhibited more neo-epidermis and abundant new blood vessel formation (Fig. 3C). On the contrary, the epidermis and blood vessels were insufficiently observed in control wounds and the wounds treated with miR-21 inhibitor MVs (Fig. 3C). Vascular endothelial growth factor (VEGF) is a signaling protein well-known for its stimulatory effect on vessel formation (Jiang et al., 2016; Spuul et al., 2016). Treatment with MVs expressing miR-21 mimic showed substantial expression of VEGF (Fig. 3D). These *in vivo* data collectively suggested miR-21 from keratinocytes-derived MVs would accelerate wound healing by promoting angiogenesis.

4.4. MV miR-21 facilitated fibroblast differentiation

After showing the *in vivo* effect of miR-21 of keratinocyte-derived MVs on the healing of the cutaneous wound, we studied the underlying molecular mechanism of miR-21 action. We determined whether miR-21 of keratinocyte-derived MVs would affect fibroblast-to-myofibroblast differentiation which may drive effective wound closure. Masson staining was used to detect the fibroblast proliferation and myofibroblasts differentiation. As showed by the staining, vector MVs as well as miR-21 mimic MVs stimulated the fibroblast differentiation and increased the proportion of myofibroblasts in a significant manner (Fig. 4A). α-SMA and N-cadherin (CDH2) are known markers of activated myofibroblasts and are stimulatory on collagen production and contraction (Black et al., 2018). In agreement with the Masson staining, treatment of cultured HFF-1 with vector MVs and miR-21 mimic MVs

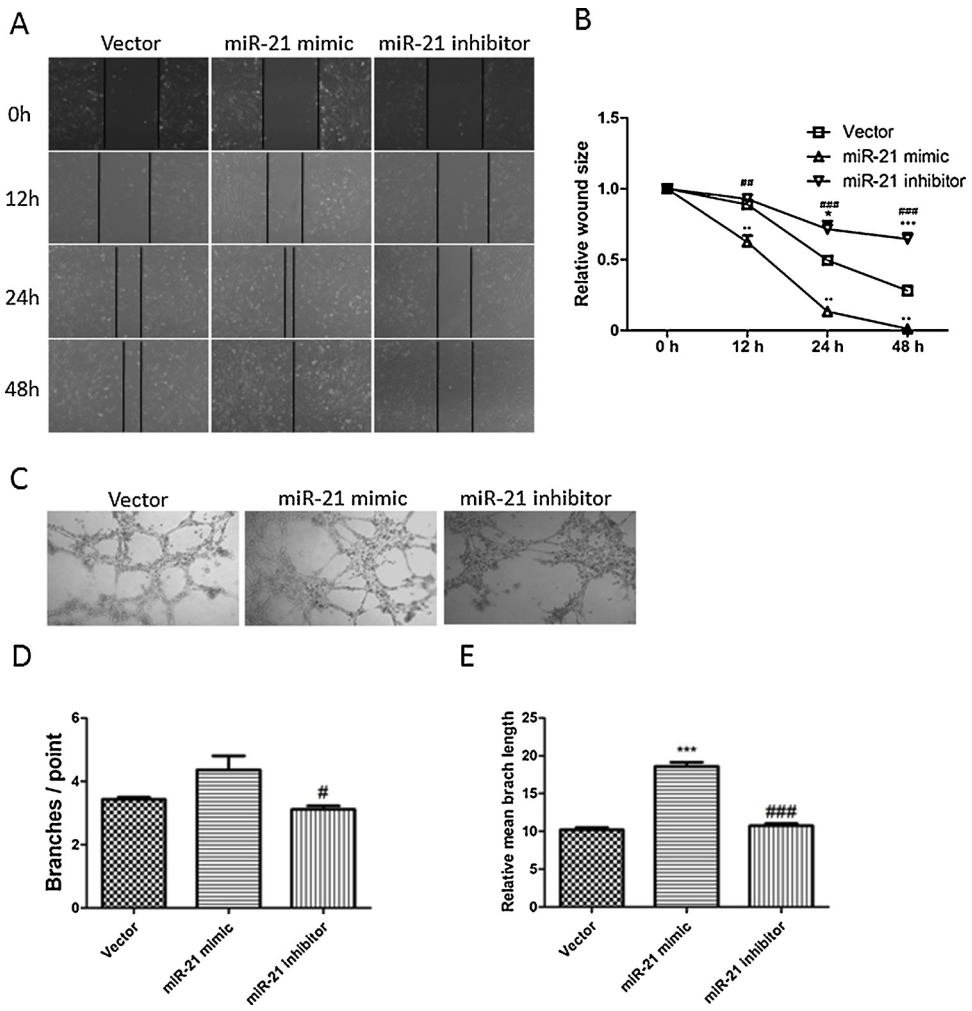

Fig. 2. Regulation of fibroblast migration and fibroblast-mediated angiogenesis by HEKa-MVs. (A) Confluent fibroblast cultures were scratch wounded and exposed to HEKa-MVs (2 μg protein / ml) containing vector, miR-21 mimic or miR-21 inhibitor for 48 h. (B) The remaining wound area was quantified by ImageJ from triplicate experiments. (C) Endothelial cells seeded on basement membrane matrix treated with concentrated (5 x) conditioned medium from HEKa-MV–treated (2 μg protein / ml) fibroblasts. Angiogenesis was quantified as (D) branches per intersection and (E) lengths of branches in randomly selected images from the culture plates. The results show mean ± SEM from triplicate experiments (***, $P < 0.001$ comparing to vector group. $^{\#}$, $P < 0.05$; $^{\#\#\#}$, $P < 0.001$ comparing to miR-21 mimic group).

significantly elevated both the gene and protein expression of α-SMA and N-cadherin (Fig. 4B, C and D). In contrast, the treatments with miR-21 inhibitor MVs did not show obvious fibroblast-to-myofibroblast differentiation in the Masson staining as well as did not elevation in α-SMA and N-cadherin expression in neither gene or protein level (Fig. 4A-D). Taken together, these results made it evident that miR-21 from keratinocyte-derived MVs would promote the switch of fibroblast to myofibroblasts.

4.5. MV miR-21 modulated pro-inflammatory interleukins and MMPs in fibroblasts

To investigate whether MV miR-21 would affect the expression of other wound healing-related genes in fibroblasts, we tested the expression of relevant cytokines, MMPs, and MMP inhibitors in mRNA and protein level. Gene expression of IL-6 and IL-8 was significantly up-regulated by miR-21 mimic MVs in the fibroblasts comparing to the control (vector MVs), whereas they were suppressed by miR-21 inhibitor MVs (Fig. 5A). Consistently, cytokine ELISA revealed that the protein levels of IL-6 and IL-8 in the culture medium of fibroblasts was also significantly increased by treatment of miR-21 mimic MVs, and decreased by treatment of miR-21 inhibitor MVs, comparing to the control (Fig. 5B). These data likely suggested MV miR-21 would play a certain modulating role in IL-6 and IL-8 expression.

We next determined whether MV miR-21 was involved in the regulation of MMP expression of fibroblast. It was found there were significant increasing mRNA expression of MMP-1 and MMP-3 in response to treatment of miR-21 mimic MVs comparing to vector MVs (Fig. 5C). Inversely, the mRNA transcripts of TIMP-3 and TIMP-4, the endogenous inhibitors to MMPs, were significantly down-regulated by miR-21 mimic MVs comparing to vector MVs (Fig. 5D). In contract, the effect was specific to miR-21 mimic because the up-regulation of MMPs and the down-regulation of TIMPs were significantly diminished with the administration of miR-21 inhibitor MVs (Fig. 5C and D). These data pointed to a notion that keratinocyte-derived miR-21 would increase MMP-1 and MMP-3 in fibroblasts by suppressing TIMPs.

4.6. MV miR-21 modulated PTEN, RECK, and the activation of MAPK/ERK signaling

Previous studies have shown that miR-21 can target PTEN and RECK in fibroblasts and activate MAPK/ERK pathway (Hu et al., 2018). We also showed in our previous publication that the modulation of MAPK/ERK pathway by keratinocyte-derived MVs was highly involved in fibroblast phenotype and function (Bi et al., 2016; Huang et al., 2015). We investigate whether miR-21 of keratinocyte-derived MVs would regulate these molecules and activate the ERK1/2 signaling pathway in the fibroblast. PTEN and RECK were significantly reduced in fibroblast after treatment of miR-21 mimic MVs in 15 min., comparing to vector MVs and MV miR-21 inhibitor (Fig. 6A and B). Consistently, treatment with MVs expressing miR-21 mimic elevated significantly phosphor-ERK1/2 in 15 min. (Fig. 6C and D).

5. Discussion

MVs play crucial roles in intercellular communication by delivering

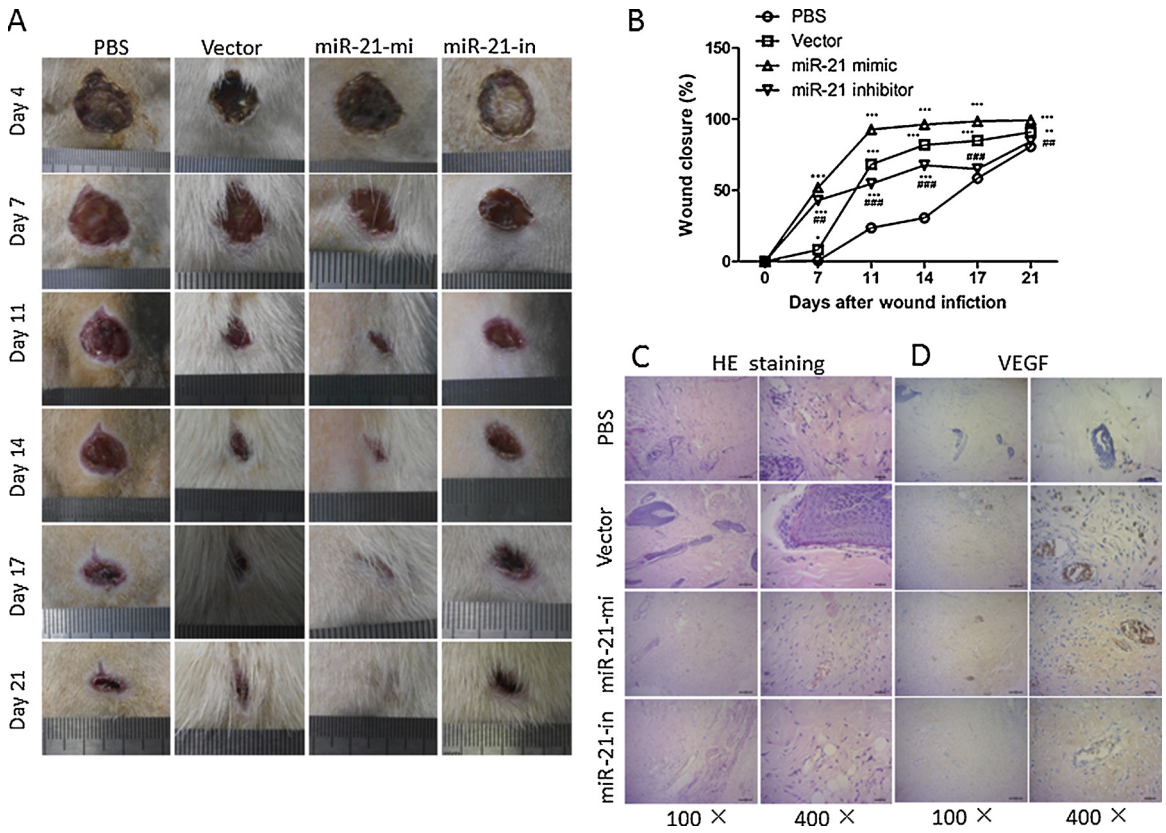

Fig. 3. MV miR-21 promoted cutaneous wound healing in diabetic rats. (A) Representative images of the cutaneous wound at different post-wounding time points. (B) The wound closure at different post-wounding time points was quantified and compared. (C) H&E staining showing the healing of the cutaneous wound, skin regeneration, and neo-vascular formation, in miR-21 mimics group. (D) IHC is showing the expression of VEGF in the cutaneous wound after different MV treatments. The results show mean ± SEM from triplicate experiments (*, $P < 0.05$; **, $P < 0.01$; ***, $P < 0.001$ comparing to PBS group. $P < 0.01$; $^{\#\#\#}$, $P < 0.001$ comparing to miR-21 mimic group).

miRNAs, mRNAs, and proteins to recipient cells (Mitchell and Tollervey, 2010). More importantly, plasma-derived MVs are gaining increasing attention to serve as diagnostic biomarkers for various diseases (Staals and Pruijn, 2010). Recently, it was reported that MVs derived from human peripheral blood PRP (platelet-rich plasma) could have therapeutic effects on diabetic wound healing in rats, implying the roles of MVs in tissues regeneration (Hashemi et al., 2017). Also, we previously reported that keratinocyte MVs promote wound healing in skin fibroblast (Huang et al., 2015). However, the cargo contents in MVs are complex and enormous (Bi et al., 2016; Huang et al., 2015). In this study, we found that the miR-21 expressed in the keratinocyte MVs may represent as a key candidate molecular in the regulation of fibroblast during wound healing.

Re-epithelization, scar formation and angiogenesis are essential processes for the restoration of normal tissue architecture after injury. Fibroblasts as the main source of the ECM proteins constitute granulation tissue in the form of myofibroblasts and provide structural integrity to the wound and even wound contraction (Govindaraju et al., 2018). Relatedly, miR-21 was reported with functions in wound healing, including cell migration, angiogenesis and re-epithelization (Wang et al., 2012; Yang et al., 2011). We previously reported that keratinocyte MV promoted skin fibroblast migration (Huang et al., 2015). In this study, treatment of HFF-1 with MVs expressing miR-21 mimic enhanced cell migrating ability of fibroblast. Furthermore, the angiogenic activity of endothelial cells, one of the key process in wound healing, were also reported to be affected by MVs in our previous publication (Asai et al., 2006; Huang et al., 2015). We showed here that miR-21-containing MVs promoted tube formation by an enhanced migration capacity of HUVEC. Our result supported the notion that miR-21 in HEKa-MVs would facilitate the angiogenic ability of endothelial cells. This was confirmed with our *in vivo* results of diabetic wound healing rat model. The HEKa derived MVs from various groups was directly injected at the wound edge. Strikingly, the wound closure was significantly accelerated and was complete after 21 days following MV-miR-21 treatment and, to a less extent, HEKa-MVs. This observation was further verified by H&E and IHC staining that the wounds treated with MV miR-21 mimic produced more neo-epidermis, abundant new blood vessels in conjunction with upregulation of VEGF. Masson staining also revealed that HEKa-MVs, as well as MV miR-21 mimic, promoted the fibroblast differentiation and increased the proportion of myofibroblasts, which are specialized for wound contraction and drives effective wound closure (Barisic-Dujmovic et al., 2010; Darby et al., 2014; Hinz, 2016). Consistently, the mRNA expression and protein levels of α-SMA and N-cadherin, known markers of activated myofibroblasts, were elevated in fibroblasts treated with HEKa-MVs or MV miR-21 mimic. These findings implicated the direct transplantation of MV miR-21 would enable skin re-epithelialization and angiogenesis of wounds, in turn, facilitating the wound healing process *in vivo*. We provide evidence suggesting the potential clinical use of HEKa-MVs in wound healing.

With these encouragingly *in vivo* findings, we further deciphered the possible mechanisms by which miR-21 regulates wound healing. MMPs were reported to facilitate re-epithelialization by cleaving different ECM or ECM-associated proteins to affect integrin-matrix adhesion (Rohani and Parks, 2015). Accumulating evidence has demonstrated that MMPs were crucial to facilitate re-epithelialization (Spuul et al., 2016). Also, RECK and TIMP3, which negatively regulates MMPs, were direct targets of miR-21 and promoted migration activity in glioma cell (Shao et al., 2017). We have previously shown that MMPs were remarkably regulated by keratinocyte MVs in skin and gingiva fibroblast

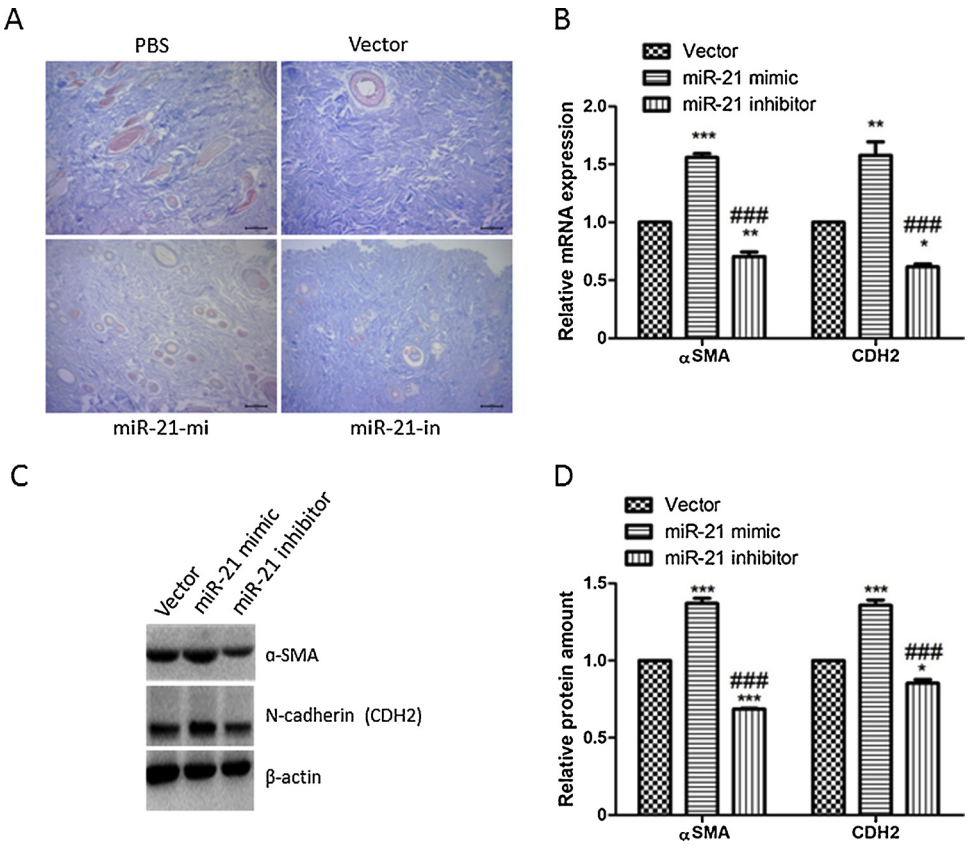

Fig. 4. The effect of HEKa-MVs on myofibroblast differentiation-related mRNA and protein expression in fibroblasts. (A) Representative images of Masson staining showing the differentiation of fibroblast into myofibroblast as stimulated by miR21 from HEKa-MVs in diabetic rats. (B) The gene expression of α-SMA and N-cadherin (CDH2) in cultured HFF-1 after treatment with different MVs for 24 h was analyzed by RT-qPCR. (C) The protein levels of α-SMA and N-cadherin (CDH2) in cultured HFF-1 after treatment with different MVs for 48 h was analyzed by western blotting. (D) The intensity of bands from western blotting was quantified and compared. The results show mean ± SEM from triplicate experiments (**, $P < 0.01$; ***, $P < 0.001$ comparing to vector group. $^{###}$, $P < 0.001$ comparing to miR-21 mimic group).

(Bi et al., 2016; Huang et al., 2015). Similarly, in this study, we determined whether miR-21 in MVs would regulate the expression of RECK and MMPs. The MMP-1 and MMP-3 mRNA levels were remarkably increased in fibroblasts with MV miR-21 mimic, while MV miR-21 inhibitor showed the opposite effects. Interestingly, the mRNA transcripts of RECK and TIMP-3 were lower following vector control and MV miR-21 mimic treatment. These data here demonstrated MV miR-21 was involved in the upregulation of MMP-1 and MMP-3 and

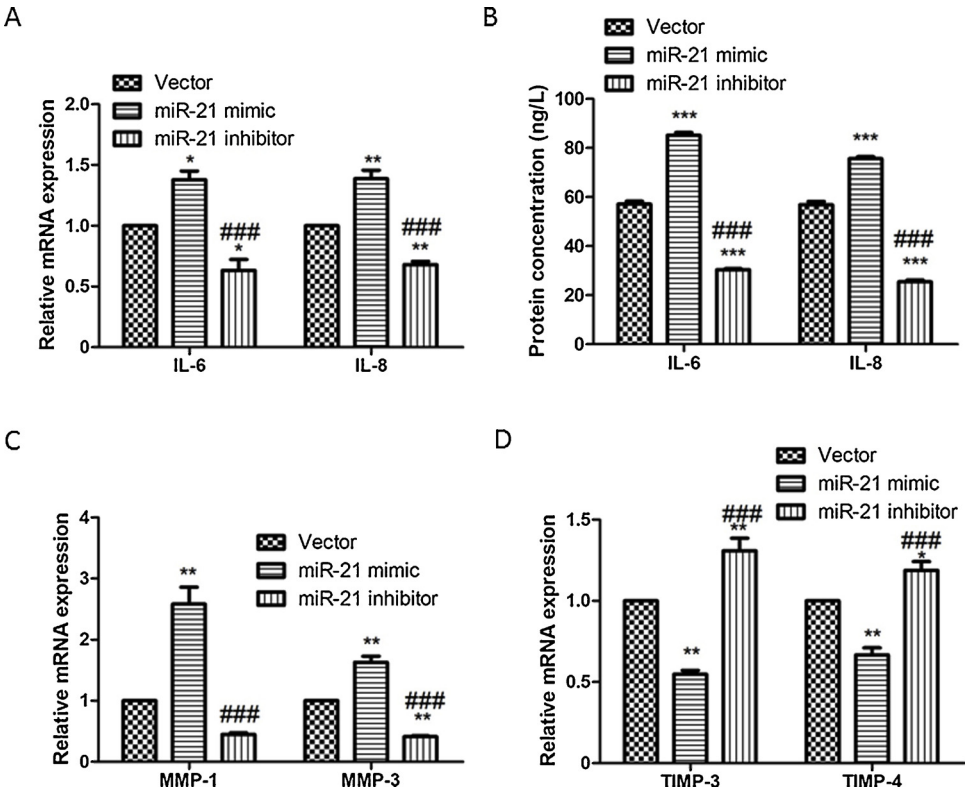

Fig. 5. The effect of HEKa-MV on the gene and protein expression of interleukins, MMPs and MMP inhibitors in fibroblasts. (A) The gene expression of IL-6 and IL-8 in cultured HFF-1 after treatment with various MVs for 24 h was analyzed by RT-qPCR. (B) The protein levels of IL-6 and IL-8 in the culture medium of HFF-1 were quantified using respective ELISA. (C) The gene expression of MMP-1 and MMP-3 in cultured HFF-1 after treatment with various MVs for 24 h was analyzed by RT-qPCR. (D) The gene expression of TIMP-3 and TIMP-4 in cultured HFF-1 after treatment with various MVs for 24 h was analyzed by RT-qPCR. The results show mean ± SEM from triplicate experiments (*, $P < 0.05$; **, $P < 0.01$; ***, $P < 0.001$ comparing to vector group. $^{###}$, $P < 0.001$ comparing to miR-21 mimic group).

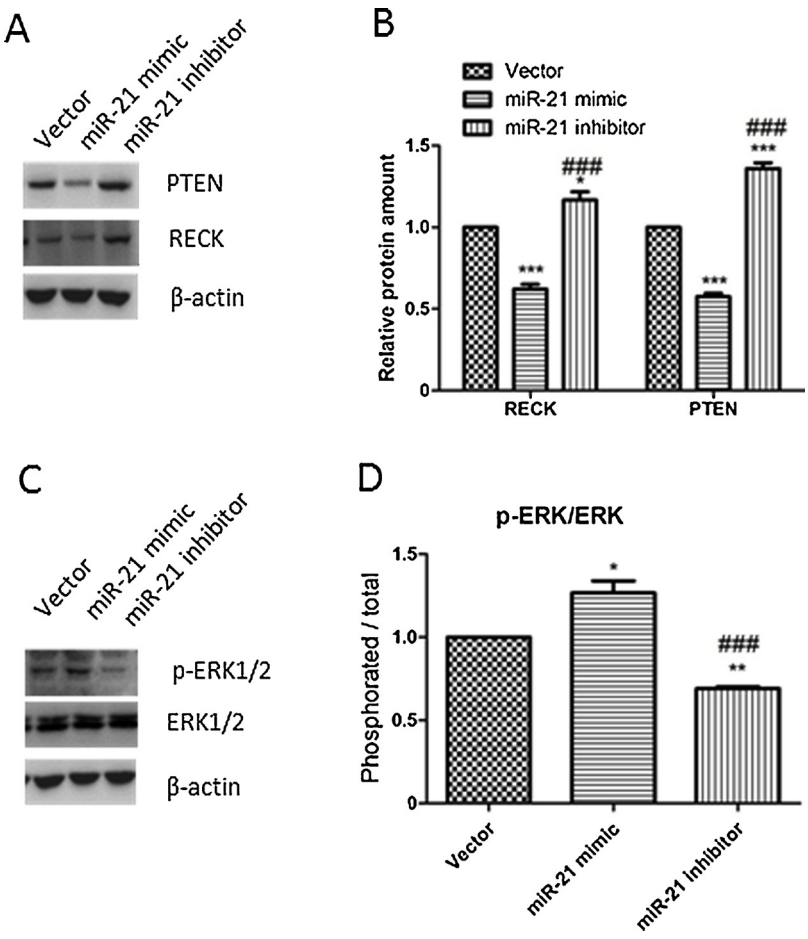

Fig. 6. HEKa-MVs regulated PTEN, RECK and ERK1/2 signaling activation in fibroblasts. (A) and (B) Fibroblasts were treated with various HEKa-MVs (2 μg protein / ml) for 15 min followed with western blotting for analysis of PTEN and RECK protein expression. (C) and (D) Fibroblasts were treated with various HEKa-MVs (2 μg protein / ml) for 15 min followed with western blotting for analysis of phosphor-ERK1/2 and ERK1/2. (B) and (D) Analysis was performed by ImageJ, and quantification was relative to cellular β-actin. The results show mean ± SEM from triplicate experiments (*, $P < 0.05$; **, $P < 0.01$; ***, $P < 0.001$ comparing to vector group. $^{###}$, $P < 0.001$ comparing to miR-21 mimic group).

suppressed RECK and TIMP3 in the fibroblast during the wound healing.

A finely-tuned inflammation was thought to be essential for the wound healing process, with the inflammatory cells releasing a variety of pro-inflammatory cytokines and chemokines that act directly on keratinocytes, fibroblasts, and endothelial cells (Eming et al., 2014). Stimulated fibroblast was demonstrated to produce cytokines such as IL-6 and IL-8 not only to amplify the wound inflammatory response but also serves as a feedback loop to support keratinocytes proliferation (Werner et al., 2007). We then examined to test whether IL-6 and IL-8 in fibroblasts would be altered by keratinocytes-derived MV miR-21. qPCR and ELISA assays indicated that MV miR-21 was indeed upregulated, implying MV miR-21 might play an important role in this paracrine feedback loop. However, additional experiments are still needed to verify this observation. PTEN which critically mediate inflammatory cytokine including IL-6 and IL-8 was recently reported as the target of miR-21 (Hu et al., 2018; Korkaya et al., 2012; Simone et al., 2011). Also, PTEN and MAPK/ERK signaling pathway were previously shown to have promoting effects on cell proliferation and migration (Chen et al., 2018; Hu et al., 2018). We showed that reduced PTEN, as well as increased phosphor-ERK1/2, was found in fibroblast treated with HEKa-MVs and, to a more extent, MV with miR-21 overexpression, whereas the miR-21 inhibitor remarkably impaired these effects. Consistently, we have shown that keratinocyte-derived MV-regulated MAPK/ERK is remarkably related to the fibroblast MMP and cytokine expression (Bi et al., 2016; Huang et al., 2015). Nevertheless, whether PTEN would be indispensable for MV miR-21 initiated fibroblast gene expression, as well as the crosstalk of PTEN and MAPK/ERK pathway in MV miR-21 treatment, need to be further addressed. Collectively, our findings demonstrated that the delivery of MV miR-21 improved fibroblast functions likely through its modulation on MMPs, which might subsequently be implicated in ECM remodeling, thus accelerated wound healing.

To summarize, the present study has provided for the first time the *in vivo* evidence suggesting the direct delivery of HEKa-MVs can be a promising therapeutic intervention for wound healing through activation of fibroblasts and angiogenic process, in which MV miR-21 is the key mediator, at least partially. The evidence supports the irreplaceable role of keratinocyte-derived MV miR-21 in skin wound healing in this study is of clinical importance.

Acknowledgments

This study was supported by grants from the National Natural Science Foundation of China (Youth Foundation; Nos. 81602742, belong to Ping Huang). The authors thank the colleagues who have contributed to this study.

References

Asai, J., Takenaka, H., Kusano, K.F., Ii, M., Luedemann, C., Curry, C., Eaton, E., Iwakura, A., Tsutsumi, Y., Hamada, H., et al., 2006. Topical sonic hedgehog gene therapy accelerates wound healing in diabetes by enhancing endothelial progenitor cell-mediated microvascular remodeling. Circulation 113, 2413–2424.

Barisic-Dujmovic, T., Boban, I., Clark, S.H., 2010. Fibroblasts/myofibroblasts that participate in cutaneous wound healing are not derived from circulating progenitor cells. J. Cell. Physiol. 222, 703–712.

Bassino, E., Vallariello, E., Gasparri, F., Munaron, L., 2017. Dermal-epidermal cross-talk: differential interactions with microvascular endothelial cells. J. Cell. Physiol. 232, 897–903.

Baumann, V., Winkler, J., 2014. miRNA-based therapies: strategies and delivery platforms for oligonucleotide and non-oligonucleotide agents. Future Med. Chem. 6, 1967–1984.

Bi, J., Dai, J., Koivisto, L., Larjava, M., Bi, L., Hakkinen, L., Larjava, H., 2018. Inflammasome and cytokine expression profiling in experimental periodontitis in the

integrin beta6 null mouse. Cytokine.
Bi, J., Koivisto, L., Owen, G., Huang, P., Wang, Z., Shen, Y., Bi, L., Rokka, A., Haapasalo, M., Heino, J., 2016. Epithelial microvesicles promote an inflammatory phenotype in fibroblasts. J. Dent. Res. 95, 680–688.
Bi, J., Koivisto, L., Pang, A., Li, M., Jiang, G., Aurora, S., Wang, Z., Owen, G.R., Dai, J., Shen, Y., et al., 2017. Suppression of alphavbeta6 integrin expression by polymicrobial oral biofilms in gingival epithelial cells. Sci. Rep. 7, 4411.
Black, M., Milewski, D., Le, T., Ren, X., Xu, Y., Kalinichenko, V.V., Kalin, T.V., 2018. FOXF1 inhibits pulmonary fibrosis by preventing CDH2-CDH11 cadherin switch in Myofibroblasts. Cell Rep. 23, 442–458.
Bloomgarden, Z.T., Drexler, A., Farley, S., 2015. New approaches to wound healing for diabetes. J. Diabetes 7, 435–436.
Brauchle, E., Bauer, H., Fernes, P., Zuk, A., Schenke-Layland, K., Sengle, G., 2017. Raman microspectroscopy as a diagnostic tool for the non-invasive analysis of fibrillin-1 deficiency in the skin and in the in vitro skin models. Acta Biomater. 52, 41–48.
Chapman, S., Liu, X., Meyers, C., Schlegel, R., McBride, A.A., 2010. Human keratinocytes are efficiently immortalized by a Rho kinase inhibitor. J. Clin. Invest. 120, 2619–2626.
Chen, C.Y., Rao, S.S., Ren, L., Hu, X.K., Tan, Y.J., Hu, Y., Luo, J., Liu, Y.W., Yin, H., Huang, J., et al., 2018. Exosomal DMBT1 from human urine-derived stem cells facilitates diabetic wound repair by promoting angiogenesis. Theranostics 8, 1607–1623.
Darby, I.A., Laverdet, B., Bonte, F., Desmouliere, A., 2014. Fibroblasts and myofibroblasts in wound healing. Clin. Cosmet. Investig. Dermatol. 7, 301–311.
Eming, S.A., Martin, P., Tomic-Canic, M., 2014. Wound repair and regeneration: mechanisms, signaling, and translation. Sci. Transl. Med. 6 265sr266.
Gao, M., Nguyen, T.T., Suckow, M.A., Wolter, W.R., Gooyit, M., Mobashery, S., Chang, M., 2015. Acceleration of diabetic wound healing using a novel protease-anti-protease combination therapy. Proc. Natl. Acad. Sci. U. S. A. 112, 15226–15231.
Geach, T., 2015. Closing the NET on impaired wound healing in diabetes mellitus. Nat. Rev. Endocrinol. 11, 443.
Ghaffari, A., Kilani, R.T., Ghahary, A., 2009. Keratinocyte-conditioned media regulate collagen expression in dermal fibroblasts. J. Invest. Dermatol. 129, 340–347.
Govindaraju, P., Todd, L., Shetye, S., Monslow, J., Pure, E., 2018. CD44-dependent inflammation, fibrogenesis, and collagenolysis regulates extracellular matrix remodeling and tensile strength during cutaneous wound healing. Matrix Biol.
Guzman-Uribe, D., Alvarado-Estrada, K.N., Pierdant-Perez, M., Torres-Alvarez, B., Sanchez-Aguilar, J.M., Rosales-Ibanez, R., 2017. Oral mucosa: an alternative epidermic cell source to develop autologous dermal-epidermal substitutes from diabetic subjects. J. Appl. Oral Sci. 25, 186–195.
Harrison, C.A., Gossiel, F., Bullock, A.J., Sun, T., Blumsohn, A., Mac Neil, S., 2006. Investigation of keratinocyte regulation of collagen I synthesis by dermal fibroblasts in a simple in vitro model. Br. J. Dermatol. 154, 401–410.
Hashemi, S.S., Mahmoodi, M., Rafati, A.R., Manafi, F., Mehrabani, D., 2017. The role of human adult peripheral and umbilical cord blood platelet-rich plasma on proliferation and migration of human skin fibroblasts. World J. Plast. Surg. 6, 198–205.
Hinz, B., 2016. The role of myofibroblasts in wound healing. Curr. Res. Transl. Med. 64, 171–177.
Hu, Y., Rao, S.S., Wang, Z.X., Cao, J., Tan, Y.J., Luo, J., Li, H.M., Zhang, W.S., Chen, C.Y., Xie, H., 2018. Exosomes from human umbilical cord blood accelerate cutaneous wound healing through miR-21-3p-mediated promotion of angiogenesis and fibroblast function. Theranostics 8, 169–184.
Huang, P., Bi, J., Owen, G.R., Chen, W., Rokka, A., Koivisto, L., Heino, J., Hakkinen, L., Larjava, H., 2015. Keratinocyte microvesicles regulate the expression of multiple genes in dermal fibroblasts. J. Invest. Dermatol. 135, 3051–3059.
Jiang, S., Li, Y., Lin, T., Yuan, L., Wu, S., Xia, L., Shen, H., Lu, J., 2016. IL-35 inhibits angiogenesis through VEGF/Ang2/Tie2 pathway in rheumatoid arthritis. Cell. Physiol. Biochem. 40, 1105–1116.
Johnson, K.E., Wilgus, T.A., 2014. Vascular endothelial growth factor and angiogenesis in the regulation of cutaneous wound repair. Adv. Wound Care (New Rochelle) 3, 647–661.
Kalucka, J., Ettinger, A., Franke, K., Mamlouk, S., Singh, R.P., Farhat, K., Muschter, A., Olbrich, S., Breier, G., Katschinski, D.M., et al., 2013. Loss of epithelial hypoxia-inducible factor prolyl hydroxylase 2 accelerates skin wound healing in mice. Mol. Cell. Biol. 33, 3426–3438.
Ke, T., Yang, M., Mao, D., Zhu, M., Che, Y., Kong, D., Li, C., 2015. Co-transplantation of skin-derived precursors and collagen sponge facilitates diabetic wound healing by promoting local vascular regeneration. Cell. Physiol. Biochem. 37, 1725–1737.
Korkaya, H., Kim, G.-i., Davis, A., Malik, F., Henry, N.L., Ithimakin, S., Quraishi, A.A., Tawakkol, N., D'Angelo, R., Paulson, A.K., 2012. Activation of an IL6 inflammatory loop mediates trastuzumab resistance in HER2+ breast cancer by expanding the cancer stem cell population. Mol. Cell 47, 570–584.
Krichevsky, A.M., Gabriely, G., 2009. miR-21: a small multi-faceted RNA. J. Cell. Mol. Med. 13, 39–53.
Lee, T.H., D'Asti, E., Magnus, N., Al-Nedawi, K., Meehan, B., Rak, J., 2011. Microvesicles as mediators of intercellular communication in cancer—the emerging science of cellular 'debris'. Paper Presented at: Seminars in Immunopathology. Springer.
Long, M., Rojo de laVega, M., Wen, Q., Bharara, M., Jiang, T., Zhang, R., Zhou, S., Wong, P.K., Wondrak, G.T., Zheng, H., et al., 2016. An essential role of NRF2 in diabetic wound healing. Diabetes 65, 780–793.
Long, S., Zhao, N., Ge, L., Wang, G., Ran, X., Wang, J., Su, Y., Wang, T., 2018. MiR-21 ameliorates age-associated skin wound healing defects in mice. J. Gene Med. 20, e3022.
Meng, Z., Zhou, D., Gao, Y., Zeng, M., Wang, W., 2018. miRNA delivery for skin wound healing. Adv. Drug Deliv. Rev. 129, 308–318.
Menon, S.N., Flegg, J.A., McCue, S.W., Schugart, R.C., Dawson, R.A., McElwain, D.L., 2012. Modelling the interaction of keratinocytes and fibroblasts during normal and abnormal wound healing processes. Proc. Biol. Sci. 279, 3329–3338.
Mitchell, P., Tollervey, D., 2010. Finding the exosome. Adv. Exp. Med. Biol. 702, 1–8.
Rohani, M.G., Parks, W.C., 2015. Matrix remodeling by MMPs during wound repair. Matrix Biol. 44-46, 113–121.
Salazar, J.J., Ennis, W.J., Koh, T.J., 2016. Diabetes medications: impact on inflammation and wound healing. J. Diab. Complicat. 30, 746–752.
Schafer, I.A., Shapiro, A., Kovach, M., Lang, C., Fratianne, R.B., 1989. The interaction of human papillary and reticular fibroblasts and human keratinocytes in the contraction of three-dimensional floating collagen lattices. Exp. Cell Res. 183, 112–125.
Scherer, S.S., Pietramaggiori, G., Matthews, J., Perry, S., Assmann, A., Carothers, A., Demcheva, M., Muise-Helmericks, R.C., Seth, A., Vournakis, J.N., et al., 2009. Poly-N-acetyl glucosamine nanofibers: a new bioactive material to enhance diabetic wound healing by cell migration and angiogenesis. Ann. Surg. 250, 322–330.
Shao, Y.Y., Zhang, T.L., Wu, L.X., Zou, H.C., Li, S., Huang, J., Zhou, H.H., 2017. AKT Axis, mir-21, and RECK play pivotal roles in dihydroartemisinin killing malignant glioma cells. Int. J. Mol. Sci. 18.
Simone, R.E., Russo, M., Catalano, A., Monego, G., Froehlich, K., Boehm, V., Palozza, P., 2011. Lycopene inhibits NF-kB-mediated IL-8 expression and changes redox and PPARγ signalling in cigarette smoke–stimulated macrophages. PLoS One 6, e19652.
Sorg, H., Tilkorn, D.J., Hager, S., Hauser, J., Mirastschijski, U., 2017. Skin wound healing: an update on the current knowledge and concepts. Eur. Surg. Res. 58, 81–94.
Souren, J.M., Ponec, M., van Wijk, R., 1989. Contraction of collagen by human fibroblasts and keratinocytes. In Vitro Cell. Dev. Biol. 25, 1039–1045.
Spuul, P., Daubon, T., Pitter, B., Alonso, F., Fremaux, I., Kramer, I., Montanez, E., Genot, E., 2016. VEGF-A/Notch-Induced podosomes proteolyse basement membrane Collagen-IV during retinal sprouting angiogenesis. Cell Rep. 17, 484–500.
Staals, R.H., Pruijn, G.J., 2010. The human exosome and disease. Adv. Exp. Med. Biol. 702, 132–142.
Steinstraesser, L., Lam, M.C., Jacobsen, F., Porporato, P.E., Chereddy, K.K., Becerikli, M., Stricker, I., Hancock, R.E., Lehnhardt, M., Sonveaux, P., et al., 2014. Skin electroporation of a plasmid encoding hCAP-18/LL-37 host defense peptide promotes wound healing. Mol. Ther. 22, 734–742.
Van Niel, G., Raposo, G., Candalh, C., Boussac, M., Hershberg, R., Cerf–Bensussan, N., Heyman, M., 2001. Intestinal epithelial cells secrete exosome–like vesicles. Gastroenterology 121, 337–349.
Wang, T., Feng, Y., Sun, H., Zhang, L., Hao, L., Shi, C., Wang, J., Li, R., Ran, X., Su, Y., et al., 2012. miR-21 regulates skin wound healing by targeting multiple aspects of the healing process. Am. J. Pathol. 181, 1911–1920.
Werner, S., Krieg, T., Smola, H., 2007. Keratinocyte-fibroblast interactions in wound healing. J. Invest. Dermatol. 127, 998–1008.
Whiting, D.R., Guariguata, L., Weil, C., Shaw, J., 2011. IDF diabetes atlas: global estimates of the prevalence of diabetes for 2011 and 2030. Diabetes Res. Clin. Pract. 94, 311–321.
Wong, S.L., Demers, M., Martinod, K., Gallant, M., Wang, Y., Goldfine, A.B., Kahn, C.R., Wagner, D.D., 2015. Diabetes primes neutrophils to undergo NETosis, which impairs wound healing. Nat. Med. 21, 815–819.
Yang, B., Suwanpradid, J., Sanchez-Lagunes, R., Choi, H.W., Hoang, P., Wang, D., Abraham, S.N., MacLeod, A.S., 2017. IL-27 facilitates skin wound healing through induction of epidermal proliferation and host defense. J. Invest. Dermatol. 137, 1166–1175.
Yang, X., Wang, J., Guo, S.L., Fan, K.J., Li, J., Wang, Y.L., Teng, Y., Yang, X., 2011. miR-21 promotes keratinocyte migration and re-epithelialization during wound healing. Int. J. Biol. Sci. 7, 685–690.
Zheng, Y., Ji, S., Wu, H., Tian, S., Wang, X., Luo, P., Fang, H., Wang, Z., Wang, J., Xiao, S., et al., 2015. Acceleration of diabetic wound healing by a cryopreserved living dermal substitute created by micronized amnion seeded with fibroblasts. Am. J. Transl. Res. 7, 2683–2693.